Heat Transfer from Horizontal Plane Heater to Potassium," *International Journal of Heat and Mass Transfer*, Vol. 26, 1983, pp. 154-156.

6 Shai, I., and Rohsenow, W., "The Mechanism of and Stability Criterion for Nucleate Pool Boiling of Sodium," ASME JOURNAL OF HEAT TRANSFER, Vol. 91, 1969, pp. 315-329.

7 Michiyoshi, I., Takenaka, N., Murata, T., Shiokawa, T., and Takahashi, O., "Boiling Heat Transfer in Potassium Layers on a Horizontal Plane Heater," *Proceedings of the ASME-JSME Thermal Engineering Joint Conference*, Vol. 1, Honolulu, 1983, pp. 207-214.

8 Subbotin, V. I., Sorokin, D. N., Ovechkin, D. M., and Kudryavtsev, A. P., "Heat Transfer in Boiling Metals by Natural Convection," Israel Program for Scientific Translation, Jerusalem, 1972.

9 Mikic, B. B., and Rohsenow, W. M., "A New Correlation of Pool-Boiling Data Including the Effect of Heating Surface Condition," ASME JOURNAL OF HEAT TRANSFER, Vol. 91, 1969, pp. 205-211.

10 Bonilla, C. F., Wiener, M., and Bilfinger, H., "Pool Boiling Heat Transfer of Potassium," *Proc. High-Temp. Liquid Metal Heat Transfer Technology Meeting*, Vol. 1, O.R.N.L.-3605, 1963, pp. 286-309.

Heat Transfer in an Annular Two-Phase Flow

F. Dobran[1]

Nomenclature

A = flow cross-sectional area, $\pi D^2/4$
Bo = buoyancy number, $1-\rho_g/\rho_l$
Ca = capillary number, $\mu_l^2/(\rho_l D\sigma)$
C_E = entrainment parameter, $\dot{m}_d/A\rho_l u_c$
C_p = specific heat at constant pressure
$D;D^+$ = tube internal diameter, $\rho_l Du^*/\mu_l$
E = fraction of the total liquid flow which is entrained
f = friction factor
g = gravitational constant
G = mass flux
h = heat transfer coefficient
k = thermal conductivity
$\dot{m}$ = mass flow rate
N_l = two-phase Grashof number, $(gD^3\rho_l(\rho_l-\rho_g)/\mu_l^2)^{1/2}$
Nu_δ = Nusselt number, $h\delta/k_l$
P = pressure
Pr = Prandtl number, $\mu C_p/k$
$\mathrm{Pr}_{\mathrm{eff}}$ = effective Prandtl number for the wavy layer region of the film, $\mu_{\mathrm{eff}}/\rho_l\epsilon_{\mathrm{eff}}$
Pr_{lt} = turbulent Prandtl number for the continuous layer region of the liquid film, ϵ_m/ϵ_h
q = heat flux
Re_c = Reynolds number, $u_c\rho_c D/\mu_g$
Re_l = film Reynolds number, $4W^+$
S = entrainment parameter, $\tau_i\delta/\sigma$
$T;T^+$ = temperature; $C_{pl}\rho_l u^*(T_w-T)/q_w$
$u;u_c$ = axial film velocity; superficial gas velocity, $A_c u_g/A$
u^* = shear velocity, $(|\tau_w|/\rho_l)^{1/2}$
u^+ = dimensionless film velocity, u/u^*
W^+ = dimensionless film flow-rate, $\int_0^{\delta^+} u^+ dy^+ = \mathrm{Re}_l/4$
We = Weber number, $\frac{\rho_G u_c^2 D}{\sigma}\left(\frac{\mathrm{Bo}}{1-\mathrm{Bo}}\right)^{1/3}$
x = quality
$y;y^+$ = distance from the tube wall; $\rho_l u^* y/\mu_l$
z = distance along the tube

Greek Symbols

α_c = core void fraction, $A_g/(A_g+A_d)$
β = interfacial shear stress parameter, defined by equation (2)
ϵ = fraction of total flow flowing as entrained liquid
$\delta;\delta^+$ = film thickness; $\rho_l\delta u^*/\mu_l$
$\delta_c;\delta_c^+$ = wave crests thickness, $\rho_l\delta_c u^*/\mu_l$
$\delta_l;\delta_l^+$ = continuous liquid layer thickness; $\rho_l\delta_l u^*/\mu_l$
$\epsilon_m;\epsilon_h$ = turbulent diffusivities for momentum and heat
$\mu;\nu$ = viscosity, μ/ρ
ρ = density
σ = surface tension
τ = shear stress

Subscripts

c = pertains to the core
d = pertains to liquid droplets in the core
eff = effective
g = pertains to the gas phase
i = liquid film-gas core interface
l = pertains to the liquid phase
sat = saturation value
w = wall
wl = pertains to the wavy layer

1 Introduction

The two-phase vertical annular flow pattern occurs in many situations of practical interest and consists of a liquid film adjacent to the channel wall and a core which consists of liquid droplets entrained in the gas phase. The interface between the liquid film and the dispersed core region is covered by a complex system of waves, and the wave structure depends on the volumetric fluxes of the two phases [1-3]. This rather complex flow pattern has been under investigation for many years and little progress has been achieved in its analytical modeling.

In modeling of the liquid film, it has been a common practice to assume that the turbulence structure in the film is identical to the structure of a single-phase turbulent pipe flow at the equivalent distances from the pipe wall; and the effects of waves on the hydrodynamic and heat transfer processes are neglected [4]. It is possible that this assumption in turbulence modeling of the liquid film is responsible for considerable overprediction of heat transfer rate across the liquid film [4, 5]. The experimental data in [2, 3, 6] show that the liquid film consists of a continuous liquid layer region close to the tube wall and of a wavy layer region close to the liquid film-dispersed core interface. Based on the experimental data of Ueda and Tanaka [2], Ueda and Nose [3], and Chien and Ibele [6], Dobran [7] has deduced an effective wavy layer region diffusivity and integrated the two-layer liquid film structure into an annular flow model for the prediction of hydrodynamics and heat transfer rate. The resulting two-layer liquid film hydrodynamic and heat transfer model gives lower rates of heat transfer than the single-layer model in which the turbulence is assumed to be identical to the single-phase turbulent pipe flow. At equivalent distances from the channel wall, the new model also gives lower values for effective turbulence diffusivities than the single liquid layer model.

In this paper, the results from the further development of the annular two-phase flow model with heat transfer are presented by accounting in the model for the entrainment of liquid droplets in the gas phase. It is shown that the effect of entrainment on the hydrodynamics and heat transfer can be significant and that the entrainment correlations should be used with caution, especially if they were developed on a basis of particular annular flow model.

2 Hydrodynamic and Heat Transfer Model

2.1 Hydrodynamics. An annular-dispersed two-phase

[1]Department of Mechanical Engineering, Stevens Institute of Technology, Hoboken, N.J. 07030, Assoc. Mem. ASME

Contributed by the Heat Transfer Division for publication in the JOURNAL OF HEAT TRANSFER. Manuscript received by the Heat Transfer Division August 25, 1983.

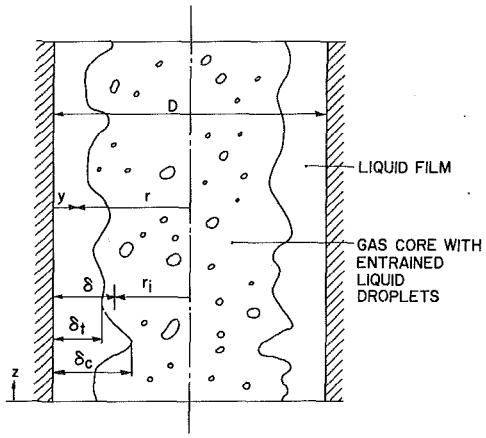

Fig. 1 An annular-dispersed, two-phase flow pattern

flow pattern in a vertical tube in upflow is illustrated in Fig. 1. It consists of a liquid film adjacent to the tube wall and of a gas core with entrained liquid droplets. The average film thickness is represented by δ; δ_t is the continuous liquid layer thickness; and $\delta_c - \delta_t$ is the wavy layer thickness. By eliminating the pressure gradient between the one-dimensional form of momentum equations for a two-phase mixture and for the liquid film, assuming that the liquid film momentum equation adequately represents the state of the film in the entire (continuous and wavy layer) thickness δ, neglecting the liquid and gas core inertia effects and momentum transport through the liquid film-core interface, and by assuming that the core consists of a homogeneous mixture of gas and liquid droplets, it is possible to derive the following equation [7, 8]

$$-\alpha_c\left(1-\frac{\delta^+}{D^+}\right)\frac{N_l^2}{D^{+3}}\delta^+ + \beta\frac{N_l^{4/3}}{\mathrm{Bo}^{1/3}(D^+)^2\left(1-\frac{2\delta^+}{D^+}\right)} - 1 = 0 \tag{1}$$

where the interfacial shear parameter β is defined as follows

$$\beta \equiv \frac{|\tau_i|}{[g^2(\rho_l-\rho_g)\mu_l^2]^{1/3}} = \frac{\tau_i}{\tau_w}\left(\frac{D^{+2}}{N_l^{4/3}}\right)\mathrm{Bo}^{1/3} \tag{2}$$

The two-layer liquid film structure enters into the hydrodynamic model through a correlation for the continuous liquid layer thickness

$$\frac{\delta_t^+}{D^+} = 140\, N_l^{0.433}\, \mathrm{Re}_c^{-1.35} \tag{3}$$

an effective momentum diffusivity for the wavy layer

$$\left(\frac{\mu_{\mathrm{eff}}}{\mu_l}\right)_{wl} = 1 + 1.6\times 10^{-3}(\delta^+ - \delta_t^+)^{1.8} \tag{4}$$

and the assumption that in the continuous layer region the turbulent velocity profile (or turbulence structure) is identical to the universal velocity profile of single phase flow [7]. For thin liquid films, the turbulent momentum equation may be written as

$$\frac{\tau}{\tau_w} = 1 - \left(1-\frac{r_i}{\tau_w}\right)\frac{y^+}{\delta^+} \tag{5}$$

and utilizing

$$\tau = \mu_{\mathrm{eff}}\frac{\partial u}{\partial y} \tag{6}$$

it is possible to combine these equations with the universal velocity profile in the continuous liquid layer region of the film to yield the liquid film flow rate, i.e.,

$$W^+ = \frac{\mathrm{Re}_l}{4} = \int_0^{\delta^+} u^+ dy^+ = W^+(\delta_t^+) + (\delta^+ - \delta_t^+)\left\{u^+(\delta_t^+) + \frac{(\delta^+ - \delta_t^+)}{2\left(\frac{\mu_{\mathrm{eff}}}{\mu_l}\right)_{wl}}\left[1-\left(1-\frac{\tau_i}{\tau_w}\right)\frac{\delta^+ + 2\delta_t^+}{3\delta^+}\right]\right\} \tag{7}$$

where Re_l is the liquid film Reynolds number and $u^+(\delta_t^+)$ and $W^+(\delta_t^+)$ are given in [7].

2.2 Heat Transfer. The heat flux rate in the film can be expressed by the usual equation

$$q = -(k_l + \rho_l C_{pl}\epsilon_h)\frac{\partial T}{\partial y} \tag{8}$$

and can be nondimensionalized as follows:

$$\frac{\partial T^+}{\partial y^+}\left(\frac{1}{\mathrm{Pr}_l} + \frac{1}{\mathrm{Pr}_{lt}}\frac{\epsilon_m}{\nu_l}\right) = \frac{\partial T^+}{\partial y^+}\left(\frac{\mu_{\mathrm{eff}}}{\mu_l}\right)\frac{1}{\mathrm{Pr}_{\mathrm{eff}}} = \frac{q}{q_w} \tag{9}$$

where $\mathrm{Pr}_l = \mu_l C_{pl}/k_l$ is the molecular Prandtl number, $\mathrm{Pr}_{lt} = \epsilon_m/\epsilon_h$ is the turbulent Prandtl number, $\mathrm{Pr}_{\mathrm{eff}} = \mu_{\mathrm{eff}}/\rho_l\epsilon_{\mathrm{eff}}$ is the effective Prandtl number and ϵ_m and ϵ_h are turbulent momentum and heat diffusivities, respectively. The turbulent momentum diffusivities follow from the development in section 2.1 and are given in [9]. Also, by neglecting the convective energy transport along the liquid film, it is possible to set $q/q_w = 1$ in equation (9) and integrate this equation from $y^+ = 0$ to $y^+ < \delta^+$ to obtain the temperature distribution in the liquid film [9].

Using equation (13) in the definition of Nusselt number, we thus obtain

$$\mathrm{Nu}_\delta \equiv \frac{q_w\delta}{(T_w - T(\delta))k_l} = \frac{\mathrm{Pr}_l\delta^+}{T^+(\delta^+)} \tag{10}$$

Notice that in the wavy layer region of the liquid film, the heat transfer process is represented by an effective diffusivity and is not split into viscous and turbulent parts as in the continuous liquid layer region. The reason for this is that the diffusivity represented by equation (4) represents the turbulent state of a *two-phase* mixture, and a split into viscous and turbulent parts as in a single phase flow situation does not appear to be physically realistic.

The hydrodynamic and heat transfer models described above are not complete until specifications for Re_c, α_c, and β are made. These specifications are, therefore, considered next.

2.3 Closure of the Hydrodynamic and Heat Transfer Model. The core void fraction α_c of a homogeneous annular-dispersed flow can be expressed as follows [10]

$$\alpha_c = \frac{1}{1+(1-\mathrm{Bo})\frac{\epsilon}{x}} \tag{11}$$

whereas the core Reynolds number Re_c follows from the definition, i.e.,

$$\mathrm{Re}_c \equiv \frac{u_c\rho_c D}{\mu_g} = \frac{x\,GD\left(1+\frac{\epsilon}{x}\right)}{\mu_g} \tag{12}$$

where G is the total mass flux and ρ_c is the homogeneous density in the core, i.e.,

$$\rho_c = \alpha_c\rho_g + (1-\alpha_c)\rho_l \tag{13}$$

The interfacial friction parameter β can be expressed in terms of the pressure gradient, or if this is not available, in terms of the interfacial roughness correlation [4, 11]. Neglecting the inertia effect in the core and the momentum transfer through the liquid film-core interface, the pressure gradient becomes

$$-\frac{dP}{dz}=\frac{2\tau_i}{\frac{D}{2}-\delta}+g\rho_c \tag{14}$$

Combining equations (2), (13), and (14) yields

$$\beta=\frac{\left(1-\frac{2\delta^+}{D^+}\right)N_l^{2/3}}{4\ \mathrm{Bo}^{2/3}}\left\{\frac{-\frac{dP}{dz}}{\rho_l g}-[(1-\alpha_c)+\alpha_c(1-\mathrm{Bo})]\right\} \tag{15}$$

When the pressure gradient is not available, the parameter β can be expressed in terms of an interfacial roughness correlation [4, 11]. This correlation supplies the interfacial friction factor f_i in the equation

$$\tau_i\equiv\frac{1}{2}f_i\rho_c u_c^2 \tag{16}$$

in terms of the core Reynolds number Re_c and film thickness δ, i.e.,

$$f_i=0.079\ \mathrm{Re}_c^{-0.25}\left(1+\frac{24}{(1-\mathrm{Bo})^{1/3}}\frac{\delta^+}{D^+}\right) \tag{17}$$

Combining equations (2), (12), (13), (16), and (17), we obtain

$$\beta=0.079\ \mathrm{Re}_c^{1.75}\left(1+\frac{24}{(1-\mathrm{Bo})^{1/3}}\frac{\delta^+}{D^+}\right)\left(\frac{\mu_g}{\mu_l}\right)^2\frac{\mathrm{Bo}^{1/3}}{2N_l^{4/3}[\alpha_c(1-\mathrm{Bo})+(1-\alpha_c)]} \tag{18}$$

For the entrainment correlation, three models will be considered. The simplest model assumes no entrainment and corresponds to $\alpha_c=1$, the second model is due to Whalley and Hewitt [11], and the third model is due to Ishii and Mishima [12].

The entrainment correlation of Whalley and Hewitt [11] is expressed in terms of the parameter C_E as a function of the independent parameter S, and when use is made of the definitions of $\dot{m}_d=\rho_l u_d A_d$, $u_c=A_c u_d/A$ and $\alpha_c=(A_c-A_d)/A_c$, these parameters can be transformed into the following form

$$\frac{C_E}{\rho_l}=1-\alpha_c \tag{19}$$

$$S=\beta\frac{N_l^{4/3}}{\mathrm{Bo}^{1/3}}\frac{\delta^+}{D^+}\mathrm{Ca} \tag{20}$$

The parameter Ca is the capillary number and represents a ratio of viscous to surface tension forces. It is important to note that Whalley's and Hewitt's entrainment correlation was determined from Hewitt's [13] annular flow model and experimental data. This model assumes that the turbulent velocity profile in the film is identical to the single-phase turbulent velocity profile in a tube. The data used to obtain the correlation pertain to air-water and stream-water mixtures, and the correlation is valid under a hydrodynamic equilibrium condition in which the local entrainment is balanced by the local droplets deposition onto the liquid film.

The entrainment correlation of Ishii and Mishima [12] is based on the low-pressure air-water data and for a hydrodynamic equilibrium condition. This correlation is expressed by

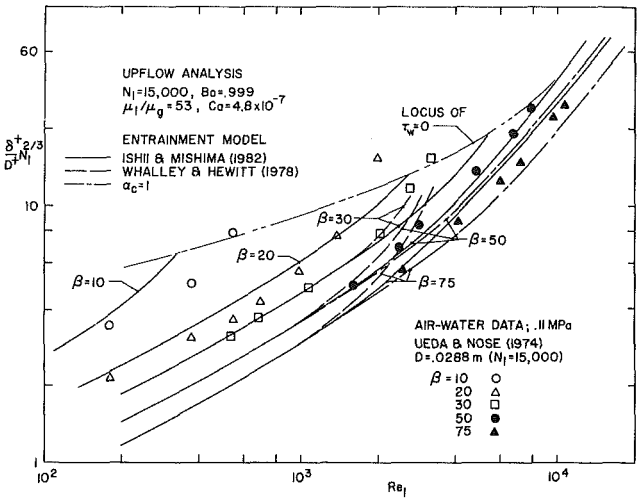

Fig. 2 Relationship between the predicted and experimental values of the liquid film thickness in upflow

$$E=\tanh\left[7.25\times10^{-7}\mathrm{We}^{1.25}\left(\frac{4W^+}{1-E}\right)^{0.25}\right] \tag{21}$$

where E is the fraction of the total liquid flow that is entrained, and We is the Weber number. Using equations (12), (13) and the definition of capillary number, it follows that

$$\mathrm{We}=\mathrm{Re}_c^2\mathrm{Bo}^{1/3}(1-\mathrm{Bo})^{2/3}\left(\frac{\mu_g}{\mu_l}\right)^2\frac{\mathrm{Ca}}{[1-\alpha_c\mathrm{Bo}]^2} \tag{22}$$

whereas by utilizing the definitions of E, ϵ, $\dot{m}_{lf}=\pi D\mu_l W^+$, and equation (12), it can be shown that

$$\frac{\epsilon}{x}=\frac{E}{(1-E)\frac{\mathrm{Re}_c}{4W^+}\frac{\mu_g}{\mu_l}-E} \tag{23}$$

and thus from equation (11), the core void fraction α_c can be determined.

The entrainment correlations expressed by equations (19) and (20), or by (21), (22) and (23) are similar in the sense that they both depend on the same parameters although this dependence is functionally very different. It is important to note that the entrainment correlation in [12] assumes that the mechanism of entrainment is the shearing of roll waves by the streaming gas velocity and that it is not produced from any specific model of the liquid film.

Equations (1-4), (7), (11-13), (15) or (18), (19) and (20) or (21), (22) and (23) yield a closed system of equations for the conditions of no phase change and in hydrodynamic equilibrium. The latter condition is assumed only in the entrainment correlations. The independent parameters of the model are buoyancy number Bo; viscosity ratio μ_g/μ_l; two-phase Grashof number N_l; capillary number Ca; molecular Prandtl number Pr_l; turbulent Prandtl number in the continuous layer region of the liquid film Pr_{ll}; and the effective Prandtl number in the wavy layer region of the film, $\mathrm{Pr}_{\mathrm{eff}}$.

3 Results and Discussion

The hydrodynamic and heat transfer model presented in the previous section for the case without accounting in the model for entrainment is compared with the experimental data by Dobran [7]. This comparison is shown to be very reasonable for vertical upflow, vertical downflow, and horizontal flow. It is also shown that the two-layer liquid film model of turbulence gives lower rates of heat transfer than the single-layer model with single-phase flow turbulent velocity profile.

Figure 2 illustrates the relationship between film thickness

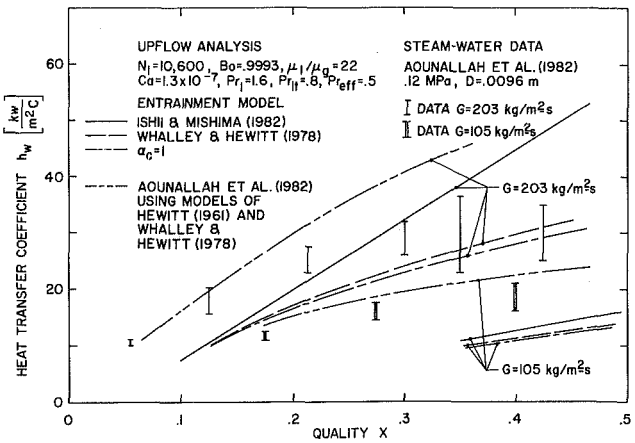

Fig. 3 Comparison between experimental and predicted heat transfer coefficients using *dP/dz* from experiment

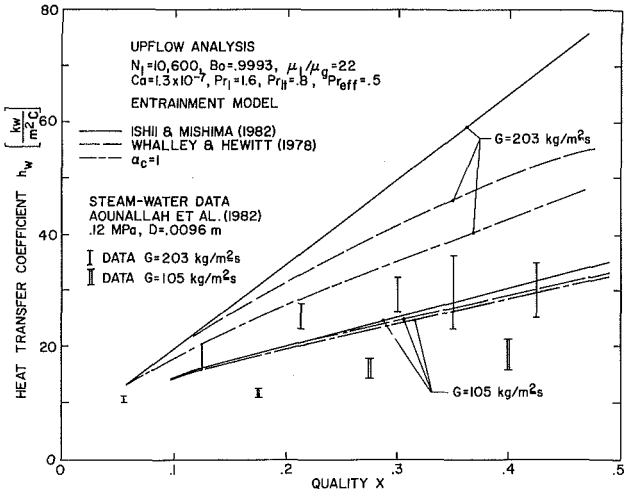

Fig. 4 Comparison between experimental and predicted heat transfer coefficients

and film Reynolds number as a function of the interfacial parameter β for vertical upflow. Also shown in this figure are the air-water data of Ueda and Nose [3] and the analytical predictions using three different entrainment models discussed in the previous section. At low β and film Reynolds numbers, all entrainment models do not affect the film thickness–Reynolds number distribution, and the accord with data is very reasonable except close to the locus of zero value of the wall shear stress ($\tau_w = 0$) where the assumed turbulence model in the film is not expected to apply. At high β and Re_l, however, the assumption that there is no entrainment in the core is not very reasonable, and a better comparison between the analysis and experiment is achieved when an account is taken in the analysis for entrainment. Note that an increase in the mean film thickness with an increase of the entrainment for fixed values of β results from the decrease of the continuous liquid layer thickness as seen from equations (3), (4), (7), and (12). As can be also seen in Fig. 2, the use of Ishii's and Mishima's entrainment correlation in the present analysis gives superior results than that due to Whalley and Hewitt. The latter entrainment correlation is found very reasonable when used in conjunction with the annual flow model of Hewitt [13].

Figures 3 and 4 illustrate the comparison between predicted and experimental values of local heat transfer coefficients as a function of quality for steam-water upflow close to the hydrodynamic equilibrium condition for two different mass fluxes. In Fig. 3, the analysis is based on the experimental value of pressure gradient, and β was, therefore, computed from equation (15), whereas in Fig. 4, β was computed from equation (18). Both of these figures also illustrate the predictions utilizing different entrainment correlations.

The accord between analysis and experiment in Fig. 3 is superior to that of Fig. 4 only at a high value of mass flux, and Whalley's and Hewitt's entrainment correlation gives slightly better heat transfer results than that of Ishii and Mishima. Lower qualities correspond to higher film Reynolds numbers, and at higher qualities that correspond to $Re_l < 2000$, the predicted heat transfer coefficients are overestimated. A possible reason for this overprediction is that the heat transfer analysis presented in section 2.2 neglects the convective energy transport along the film and thus underestimates the liquid film thermal resistance. An annular flow model in which no account is taken for entrainment leads to lower heat transfer coefficients than the one with the entrainment. This is physically realistic, since the entrainment in the analysis leads to thinner liquid films and, therefore, to lower resistance of heat transfer.

Using the annular flow model of Hewitt [13] and the entrainment correlation of Whalley and Hewitt [11], Aounallah et al. [14] carried out the analytical prediction of their experimental data, and their results are also illustrated in Fig. 3. Their prediction of heat transfer coefficient is higher than in the present analysis, and at higher Reynolds numbers (lower qualities) it is somewhat better than the prediction of the present model. At lower Reynolds numbers or higher qualities, the present model compares more favorably with the experimental data.

A better comparison of the present model with the experimental data of steam–water can be achieved by modifying the values of the turbulent Prandtl number Pr_{lt} in the continuous liquid layer region of the film and the value of effective Prandtl number Pr_{eff} in the wavy layer region of the film. In the results shown in Figs. 3 and 4, the former value is set at 0.8 and the latter at 0.5, since these values were found to be most reasonable in [7]. The value of $Pr_{eff} = 0.5$ signifies that the interfacial waves transfer their heat energy over a distance which is larger than the thickness of the wavy layer.

The disparities between analytical predictions and experimental data in Figs. 3 and 4 reflect (*i*) the uncertainty of the interfacial roughness correlation expressed by equation (17), (*ii*) the uncertainty of turbulence modeling in the film, (*iii*) the uncertainty of entrainment models, and (*iv*) the neglect of convective energy transport in the film.

4 Conclusions

An analytic model was presented for modeling annular-dispersed two-phase flows with heat transfer in a vertical upflow. The analysis incorporated a two-layer liquid film turbulence structure and was supplemented by using two recent developments for the entrainment of liquid droplets in the core. It is shown that the prediction of hydrodynamics and heat transfer from the model depends on the model for entrainment, and that the best prediction is achieved with an entrainment correlation that was not developed from any specific model of the liquid film. The two-layer liquid film turbulence structure also yielded the predicted heat transfer coefficients that are in better agreement with the experiments that those predicted by utilizing the single-layer model and turbulent velocity profile of single-phase flow.

References

1 Dukler, A. E., "Characterization, Effects and Modeling of the Wavy Gas-Liquid Interface," *Progress in Heat and Mass Transfer*, Vol. 6, Pergamon Press, New York, 1972, pp. 207–234.

2 Ueda, T., and Tanaka, T., "Studies of Liquid Film Flow in Two-Phase Annular and Annular-Mist Flow Regions; Part 1, Downflow in a Vertical Tube," *Bulletin JSME*, Vol. 17, 1974, pp. 603–613.

3 Ueda, T., and Nose, S., "Studies of Liquid Film Flow in Two-Phase

Annular and Annular-Mist Flow Regions; Part 2, Upflow in a Vertical Tube," *Bulletin JSME*, Vol. 17, 1974, pp. 614-624.

4 Bergles, A. E., Collier, J. G., Delhaye, J. M., Hewitt, G. F., and Mayinger, F., *Two-Phase Flow and Heat Transfer in Power and Process Industries*, Hemisphere, New York, 1981.

5 Butterworth, D., and Hewitt, G. F., *Two-Phase Flow and Heat Transfer*, Oxford University Press, 1977.

6 Chien, S., and Ibele, W., "Pressure Drop and Liquid Film Thickness of Two-Phase Annular and Annular-Mist Flows," ASME JOURNAL OF HEAT TRANSFER, 1964, pp. 80-96.

7 Dobran, F., "Hydrodynamic and Heat Transfer Analysis of Two-Phase Annular Flow with a New Liquid Film Model of Turbulence," *International Journal of Heat and Mass Transfer*, Vol. 26, 1983, pp. 1159-1171.

8 Dobran, F., "Condensation Heat Transfer and Flooding in a Counter-Current Subcooled Liquid and Saturated Vapor Flow," *Thermal Hydraulics in Nuclear Power Technology*, edited by K. H. Sun and S. C. Yao, ASME, New York, 1981, pp. 9-19.

9 Dobran, F., "Heat Transfer in an Upflowing Annular-Dispersed Flow," *Interfacial Transport Phenomena*, edited by J. C. Chen and S. G. Bankoff, ASME, New York, 1983, pp. 93-99.

10 Wallis, G. B., *One-Dimensional Two-Phase Flow*, McGraw-Hill, New York, 1969.

11 Whalley, P. B., and Hewitt, G. F., "The Correlation of Liquid Entrainment Fraction and Entrainment Rate in Annular Two-Phase Flow," AERE-R9187 Report, July, 1978.

12 Ishii, M., and Mishima, K., "Liquid Transfer and Entrainment Correlation for Droplet-Annular Flow," *Seventh International Heat Transfer Conference*, Vol. 5, 1982, pp. 307-312.

13 Hewitt, G. F., "Analysis of Annular Two-Phase Flow: Application of the Dukler Analysis to Vertical Upward Flow in a Tube," UKAEA Report No. AERE-R-3680, 1961.

14 Aounallah, Y., Kenning, D. B. R., Whalley, P. B., and Hewitt, G. F., "Boiling Heat Transfer in Annular Flow," *Seventh International Heat Transfer Conference*, Vol. 4, 1982, pp. 193-199.

Combined Free and Forced Convection on Vertical Slender Cylinders

M. N. Bui[1] and T. Cebeci[2]

Introduction

Flows over cylinders are usually considered to be two dimensional as long as the body radius is large compared to the boundary layer thickness. With the slender cylinders considered in this paper, the boundary layer thickness may be of the same order as the cylinder radius and the governing conservation equations must be solved for axisymmetric flows. In this case, the equations contain the transverse curvature term, which strongly influences velocity and temperature profiles, and the corresponding skin-friction and wall heat transfer as the ratio of cylinder radius to boundary layer thickness becomes smaller.

The magnitude of the transverse-curvature effect has been investigated for isothermal, laminar flows by, for example, Seban and Bond [1], Kelly [2], Stewartson [3] and Cebeci [4], and the results show, for example, that the local skin friction can be altered by an order of magnitude by a similar change in the ratio of boundary layer thickness to cylinder radius. It is evident, therefore, that the calculation of momentum and heat transfer on slender cylinders should consider the transverse curvature effect, especially in applications such as wire and fiber drawing, where accurate predictions are required and thick boundary layers can exist on slender, near-cylindrical bodies.

The results of [1-3], and of related heat transfer investigations such as that of Sparrow and Gregg [5] made use of similarity methods and power series to obtain these solutions. Reference [4], in contrast, solved the boundary layer equations in their differential form by a finite difference procedure that has been extensively tested and shown to be accurate and precise. A version of this solution procedure has been used to obtain the results presented in this paper and is described in [6]. The equations that have been solved are presented in the following section and represent conservation of mass, momentum, and energy. The buoyancy term is included in the momentum equations and the solutions correspond to the laminar forced-convection flow upwards along a vertical, slender cylinder with heat-flux boundary conditions that correspond to wall heating and cooling. The combination of free and forced convection, with the two acting both together and in opposite directions, represents an extension of free-convection solutions of Cebeci [4], which, like the present results, quantify the influence of transverse curvature in which the boundary forces aid and oppose the development of the boundary layer.

Basic Equations

We consider a steady laminar incompressible flow over a vertical cylinder of radius r_o. The boundary layer equations and their boundary conditions are well known and can be written as

$$\frac{\partial}{\partial x}(ru)+\frac{\partial}{\partial y}(rv)=0 \tag{1}$$

$$u\frac{\partial u}{\partial x}+v\frac{\partial u}{\partial y}=g_c\beta(T-T_e)+\frac{\nu}{r}\frac{\partial}{\partial y}\left(r\frac{\partial u}{\partial y}\right) \tag{2}$$

$$u\frac{\partial T}{\partial x}+v\frac{\partial T}{\partial y}=\frac{\nu}{\mathrm{Pr}}\frac{1}{r}\frac{\partial}{\partial y}\left(r\frac{\partial T}{\partial y}\right) \tag{3}$$

$$y=0,\ u=v=0,\ T=T_w;\ y=\delta,\ u=u_e,\ T=T_e \tag{4}$$

Equations (1-4) can be put into a more convenient form for solution by using the following transformation and dimensionless variables

$$d\eta=\sqrt{\frac{\bar{u}_e}{\nu x}}\frac{r}{r_o}dy,\ z=x/r_o,\ g=\frac{T-T_e}{T_w-T_e} \tag{5}$$

together with a dimensionless stream function defined by

$$\psi=(u_e\nu x)^{1/2}r_o f(z,\eta) \tag{6}$$

Introducing the above relations into equations (1-4), and with primes denoting differentiation with respect to η, we get

$$[(1+\Lambda\eta)f'']'+\frac{1}{2}ff''=\pm\mathrm{Ri}zg+z\left(f'\frac{\partial f'}{\partial z}-f''\frac{\partial f}{\partial z}\right) \tag{7}$$

$$\left[\frac{(1+\Lambda\eta)}{\mathrm{Pr}}g'\right]'+\frac{1}{2}fg'=z\left(f'\frac{\partial g}{\partial z}-g'\frac{\partial f}{\partial z}\right) \tag{8}$$

$$\eta=0;\ f=f'=0,\ g=1;\ \eta=\eta_e;\ f'=1,\ g=0 \tag{9}$$

Here Λ defines the transverse curvature parameter and Ri, the Richardson number,

$$\Lambda=2(z/R)^{1/2},\quad \mathrm{Ri}=\frac{\mathrm{Gr}}{R^2},\quad R=\frac{u_e r_o}{\nu},$$

$$\mathrm{Gr}=\frac{g_c\beta}{\nu^2}(T_w-T_e)r_o^3 \tag{10}$$

Results and Discussion

Results have been obtained for Prandtl numbers of 0.1, 1.0, and 10, for positive and negative heat transfer through the wall (i.e., heating and cooling) and as a function of the curvature parameter Λ defined in equation (10). A sample of the results is presented in Figs. 1 to 3 and the reader is referred to reference 6 for the complete set of results.

The velocity and temperature profiles of Figs. 1(*a*) and 1(*b*) correspond to wall heating and wall cooling, respectively, so

[1]Graduate student, Mechanical Engineering Department, California State University, Long Beach, Calif., Student Mem. ASME

[2]Professor, Mechanical Engineering Department, California State University, Long Beach, Calif., Mem. ASME

Contributed by the Heat Transfer Division for publication in the JOURNAL OF HEAT TRANSFER. Manuscript received by the Heat Transfer Division December 7, 1983.